15 Feb 2013

Equilibrium and Nonequilibrium Molecular Dynamics Simulations of Thermal Conductance at Solid-Gas Interfaces

Zhi Liang
Missouri University of Science and Technology, zlch5@mst.edu

William Evans

Pawel Keblinski

Recommended Citation

Z. Liang et al., "Equilibrium and Nonequilibrium Molecular Dynamics Simulations of Thermal Conductance at Solid-Gas Interfaces," *Physical Review E - Statistical, Nonlinear, and Soft Matter Physics*, vol. 87, no. 2, article no. 22119, American Physical Society, Feb 2013.
The definitive version is available at https://doi.org/10.1103/PhysRevE.87.022119

Equilibrium and nonequilibrium molecular dynamics simulations of thermal conductance at solid-gas interfaces

Zhi Liang,[1,*] William Evans,[2] and Pawel Keblinski[1,3,†]
[1]*Rensselaer Nanotechnology Center, Rensselaer Polytechnic Institute, Troy, New York 12180, USA*
[2]*Focus Center-New York, Rensselaer Polytechnic Institute, Troy, New York 12180, USA*
[3]*Department of Materials Science and Engineering, Rensselaer Polytechnic Institute, Troy, New York 12180, USA*
(Received 10 December 2012; published 15 February 2013)

The thermal conductance at solid-gas interfaces with different interfacial bonding strengths is calculated through Green-Kubo equilibrium molecular dynamics (EMD) simulations. Due to the finite size of the simulation system, the long-time integral of the time correlation function of heat power across the solid-gas interface exhibits an exponential decay, which contains the information on interfacial thermal conductance. If an adsorbed gas layer is formed on the solid surface, it is found that the solid-gas interface needs to be defined at a plane outside the adsorbed layer so as to obtain the correct result from the Green-Kubo formula. The EMD simulation result agrees very well with that obtained from nonequilibrium molecular dynamics simulations. By calculating the average solid-gas interaction time as a function of solid-gas interaction strength, we find the incident gas atoms thermalize with the metal surface much more rapidly when the surface is covered by adsorbed gas molecules.

DOI: 10.1103/PhysRevE.87.022119 PACS number(s): 47.45.−n, 34.35.+a

I. INTRODUCTION

The efficient cooling of microelectronic devices is one of the crucial challenges in the further progress of microelectronic industry. Single-phase gas cooling is the dominant thermal management technology for cooling of electrical components. Hence, the understanding of heat transfer characteristics close to the solid-gas interface is important, especially when microchannels/nanochannels are applied in the cooling of microdevices. The efficiency of heat transfer at the solid-gas interface is determined by the solid-gas interfacial thermal conductance, G_K. G_K is strongly affected by solid-gas interaction strength. However, solid-gas interactions are difficult to quantify, control, and tune in experiment. This prevents the systematic study of the effect of interfacial bonding on heat transfer. Molecular dynamics simulations provide an opportunity to systematically study the dependence of interfacial thermal conductance on interfacial binding strength. For instance, Xue *et al*. [1,2] have found the functional dependence of solid-liquid interfacial thermal conductance on the strength of the solid-liquid interactions using nonequilibrium molecular dynamics (NEMD) method. In this work, we use NEMD and equilibrium molecular dynamics (EMD) methods to investigate the dependence of G_K on solid-gas interaction strength and associated heat transfer mechanism.

While the NEMD technique is more widely used in the calculation of interfacial thermal conductance, the EMD method based on Green-Kubo formula can provide insight into the mechanisms of interfacial heat transfer [3]. The EMD technique has been successfully used to determine solid-solid [4–6] and solid-liquid [7,8] interfacial thermal conductance. To our knowledge, however, the EMD method has not been applied to determine solid-gas interfacial thermal conductance. We will show in this work that EMD and NEMD results are equivalent in the calculation of solid-gas interfacial thermal conductance. Nevertheless, the definition of solid-gas interface needs to be modified when a solid is covered by adsorbed gas molecules. This is the case when solid-gas interaction strength is high.

II. EMD AND NEMD DETERMINATION OF G_K

The model simulation systems consist of a solid Pt slab in contact with Ar gas as depicted in Fig. 1. The Pt slab is formed by nine layers of FCC (111) planes with the cross section area of 7.2 nm × 7.2 nm. The length of the gas region, L_g is 170 nm in NEMD simulations and 80 nm in EMD simulations. Periodic boundary conditions are applied in all three directions. The Lennard-Jones (LJ) 12-6 potential with parameters $\sigma = 3.41$ Å and $\varepsilon = 10.3$ meV is employed for Ar-Ar interactions [9]. The embedded-atom-method (EAM) potential [10] is used for Pt-Pt interactions. For Pt-Ar interactions, an LJ potential with parameters $\sigma_{sf} = 3.09$ Å and $\varepsilon_{sf} = 6.82$ meV [11] is used as a reference potential. To study the effect of solid-gas interaction strength on interfacial thermal conductance, we artificially change ε_{sf} to various values while keep σ_{sf} constant. The cutoff distance for all LJ interactions is 11 Å in the simulation.

All simulations are performed at 300 K and 10 bar. Under these conditions, the estimated mean free path, λ_g, of Ar atoms is about 7.0 nm [12]. Accordingly, the Knudsen number $Kn = \lambda_g/L_g$ in the model system is between 0.01 and 0.1, which belongs to the temperature jump regime in gas dynamics problems [13]. Both EMD and NEMD simulations are carried out to determine solid-gas interfacial thermal conductance.

A. NEMD simulations

The determination of solid-gas interfacial thermal conductance by NEMD simulations is straightforward. As shown in Fig. 1, we set the whole Pt slab as the heat source and the middle of the gas phase as heat sink. At the steady state, a temperature jump at the solid-gas interface, ΔT, will be obtained and the

*liangz3@rpi.edu
†keplip@rpi.edu

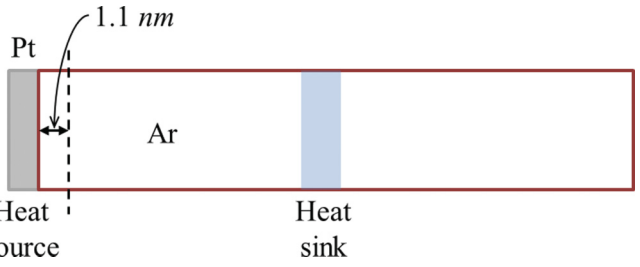

FIG. 1. (Color online) Schematic diagram of the computational cell. Periodic boundary conditions are applied in all three directions. The dashed line indicates the location of the imaginary plane which is 1.1 nm away from the Pt surface. The cross section area is 7.2 nm × 7.2 nm. The length of gas region is 170 nm in case of NEMD simulations and 80 nm in case of EMD simulations.

interfacial thermal conductance is calculated directly using

$$G_K = q/\Delta T, \tag{1}$$

where q is the heat flux across the solid-gas interface. Additionally, the thermal accommodation coefficient, α, (TAC) which quantifies the efficiency of the solid-gas energy exchange can also be obtained through NEMD simulations. In the case of monoatomic gases, TAC is defined by [14]

$$\alpha = (T_r - T_i)/(T_s - T_i), \tag{2}$$

where T_i and T_r are the temperatures of incident and reflected gas atoms, respectively, and T_s is the solid surface temperature. In the temperature jump regime, TAC relates to the interfacial thermal conductance G_K by [12]

$$G_K = 4k_B N\alpha/(2-\alpha), \tag{3}$$

where k_B is the Boltzmann constant and N is collision rate per unit area. The collision rate is a function of pressure, P, temperature, T, and the atomic mass m and given by [12]

$$N = P/\sqrt{2\pi m k_B T}. \tag{4}$$

Equations (3) and (4) allow us to evaluate the maximum theoretical value of the $G_K = 1.33$ MW/m^{2}K for $\alpha = 1$. Moreover, the simulation results of the TACs can be used to verify the G_K results. To determine T_i and T_r in Eq. (2), we set an imaginary plane 11 Å (cutoff distance of solid-gas interactions) away from the solid surface. The gas atoms passing through the imaginary plane are defined as incident or reflected atoms depending on their instantaneous velocity directions. The small distance between the plane and surface ensures the collision between the reflected gas atoms and the adjacent gas atoms is rare. The temperature of incident (or reflected) gas atoms is obtained by dividing the average kinetic energy of the incident (or reflected) atoms by $2k_B$ [12]. Furthermore, we can divide the kinetic energy of gas atoms into components whose corresponding momenta are parallel or perpendicular to the solid surface, and thus calculate the parallel and perpendicular components of TACs, which provide more information on interfacial heat transfer than G_K.

B. EMD simulations

The EMD method evaluates the interfacial thermal conductance via the Green-Kubo formula [15]

$$G_K = \frac{1}{Ak_B T^2}\int_0^\infty \langle p(t)\, p(0)\rangle dt, \tag{5}$$

where $\langle\cdots\rangle$ denotes ensemble average, A is the cross section area of solid surface, t is time, and p is the fluctuating heat power across the solid-gas interface which can be computed by

$$p(t) = dE_{\text{gas}}(t)/dt, \tag{6}$$

where E_{gas} is the internal energy of the gas phase at time t. If the solid-gas interface is defined at the solid surface, there will be no mass transport across the interface. In this case, Eq. (6) can be written as [4,5]

$$p(t) = \frac{1}{2}\sum_{i\in\text{gas}}\sum_{j\in\text{solid}} \vec{f}_{ij}\cdot(\vec{v}_i + \vec{v}_j), \tag{7}$$

where f is the interatomic force between a solid atom and a gas atom, v are atomic velocities. If however, the solid surface is covered by adsorbed gas atoms, then the adsorbed gas atoms belong to a solid rather than gas phase. Hence, it is more appropriate to define the solid-gas interface at a plane outside of the adsorbed layer. In this case, mass exchange occurs at the interface, thus we must rely on Eq. (6) to determine the heat power.

As pointed out by Barrat and Chiaruttini [7], the Green-Kubo relation shown in Eq. (5) is only valid for an infinite system where the heat capacity of the gas, $C_V \to \infty$. However, the model system in our simulation is finite. For a finite system, the G_K actually relates to the long-time integral of $\langle p(t)p(0)\rangle$ by [7]

$$G_K e^{-at_s} = \frac{1}{Ak_B T^2}\int_0^{t_s} \langle p(t)\, p(0)\rangle dt, \tag{8}$$

where $a = AG_K/C_V$, t_s is the integration time. Hence, the running integral $\int\langle p(t)p(0)\rangle dt$ will show an exponential decay at long times due to the finite size of the system. As indicated by Eq. (8), the exponential decay contains the information on G_K. In some cases, the running integral $\int\langle p(t)p(0)\rangle dt$ may contain a plateau part, which can be used to evaluate G_K. The plateau occurs if G_K is very small or C_V is very large, which makes $e^{-at} \approx 1$. However, in the case of our study the exponential decay part of the running integral is more reliable in the determination of G_K.

C. Simulation details

A velocity Verlet scheme with a time step size of 4 fs is used for integration of equations of motions [16]. The Berendsen *et al.*'s algorithm [17] with a reduced time constant of 2 ps is used to equilibrate the system to the preset temperature ($T = 300$ K). Hence, the reference ε_{sf} (6.82 meV) for Pt-Ar interaction corresponds to $0.264k_B T$. In order to study the effect of interfacial bonding on heat transfer, we vary Pt-Ar interaction strength from $0.132k_B T$ to over $5.93k_B T$. The number of gas atoms in the model system depends on the solid-gas interaction strength. With a strong surface attraction,

a considerable number of gas atoms are bonded to the surface. Thus, we increase the number of gas atoms to maintain the gas at 10 bar in all simulations. All systems are first equilibrated for 10 ns to reach the desired temperature and pressure. In the subsequent production runs, the thermostat is eliminated, and the number of atoms in the system is kept constant.

In NEMD simulations, the gas region is divided evenly into 17 bins (bin thickness equals 10 nm). The middle three bins in the gas phase belong to the heat sink region. Energy is added at a constant rate of 0.518 nW to the Pt slab and is removed at the same rate in the heat sink at each time step by velocity rescaling [18]. In all simulations the resulting heat flux is 10 MW/m^2. Each heat source-sink simulation run is first carried for 12 ns to allow the system to reach a steady state, and then it is run for an additional 100 ns for data collection and averaging.

The EMD simulation is carried out in a microcanonical ensemble. 100 ns is used to calculate the time correlation function $\langle p(t)p(0)\rangle$, up to 150 ps with a time interval of 4 fs. The interfacial thermal conductance is determined by an exponential fit of the tail of the running integral $\int \langle p(t)p(0)\rangle dt$. The uncertainties are determined from the analysis of eight independent simulation runs.

III. SIMULATION RESULTS

A. Surface coverage and solid-gas interaction time

Gas atoms exchange thermal energies with solid surfaces through solid-gas interactions/collisions. If gas atoms are adsorbed on the surface, the solid-gas interaction time will be much longer than that in the case of direct inelastic scattering. Longer interaction time leads to the more thorough thermalization of gas atoms at the surface, a higher accommodation coefficient, and thus, a higher G_K. Hence, the calculation of the number of adsorbed gas atoms per unit surface area, i.e., surface coverage, and the average solid-gas interaction time can help us understand the relation between G_K and the solid-gas interaction strength, ε_{sf}.

The surface coverage as a function of ε_{sf} at 300 K and 10 bar is determined from the EMD simulations. The results are shown in Fig. 2. If ε_{sf}/k_BT is small, which means solid-gas binding energy is small compared to kinetic energy of gas atoms, then limited adsorption is found. Figure 3(a) shows the density distribution of gas close to the solid surface in the case of $\varepsilon_{sf} = 0.264k_BT$. As ε_{sf} becomes comparable to or higher than kinetic energy of gas atoms, the surface coverage increases almost exponentially with increasing ε_{sf} until $\varepsilon_{sf} = 3k_BT$. Here the first adsorbed gas layer is formed [see Fig. 3(b)]. The dependence of surface coverage on ε_{sf} is consistent with Langmuir's adsorption theory [14]. Further increase of ε_{sf} results in the formation of the second adsorbed layer [see Fig. 3(c)]. As the solid-gas binding energy of the second layer is much smaller than that of the first layer, we observe a slow increase of surface coverage with ε_{sf} after the first gas layer fully covers the surface.

The average solid-gas interaction time is strongly correlated with the surface coverage. In the case of limited adsorption, most gas atoms bounce a few times on the surface before they are reflected to the gas phase. Accordingly, the solid-gas

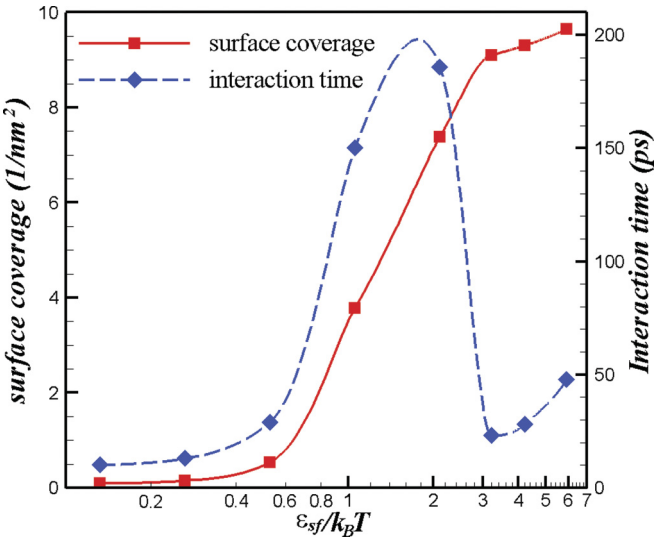

FIG. 2. (Color online) Surface coverage and average interaction time as a function of solid-gas binding strength ε_{sf} from EMD simulation of Pt-Ar system at 300 K and 10 bar. The solid and dashed lines are used to guide the eye.

interaction time is only about 10 ps as shown in Fig. 2. The formation of an adsorbed gas layer significantly increases the average solid-gas interaction time. As shown in Fig. 2, the maximum interaction time could reach more than 150 ps, which allows for the complete thermalization of gas atoms with Pt surface at room temperature [19]. Hence, highly efficient interfacial heat transfer is expected upon the formation of adsorbed Ar layer.

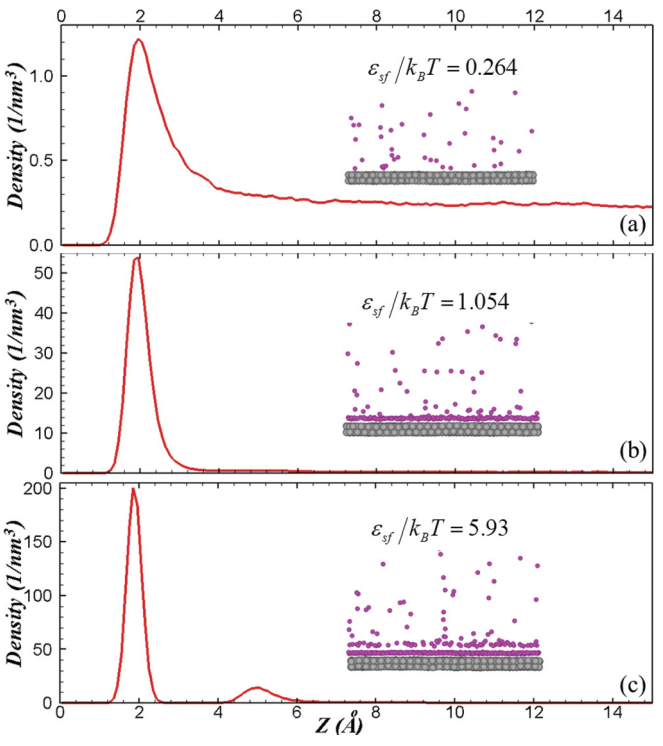

FIG. 3. (Color online) Density distribution of Ar at Pt surface for ε_{sf}/k_BT = (a) 0.264, (b) 1.05, and (c) 5.93. The insets show the snapshot of Ar atoms on Pt surface at 300 K and 10 bar.

However, if the solid-gas binding energy is much higher than the kinetic energy of gas atoms, the adsorbed Ar atoms reside on the surface for a long time, which results in virtually no exchange of the atoms between the gas phase and the adsorbed layer. In this case, the adsorbed gas atoms belong to a solid rather than gas phase. Consequently, gas phase atoms actually collide mostly with the adsorbed layer, and the solid-gas interaction time becomes shorter as shown in Fig. 2.

B. G_K at the reference ε_{sf}

We now show the results of the EMD determination of G_K at the reference solid-gas interaction strength, $\varepsilon_{sf} = 0.264 k_B T$. The corresponding time correlation function of heat power across the solid-gas interface is shown in Fig. 4(a). In the calculation, we consider two definitions of solid-gas interface.

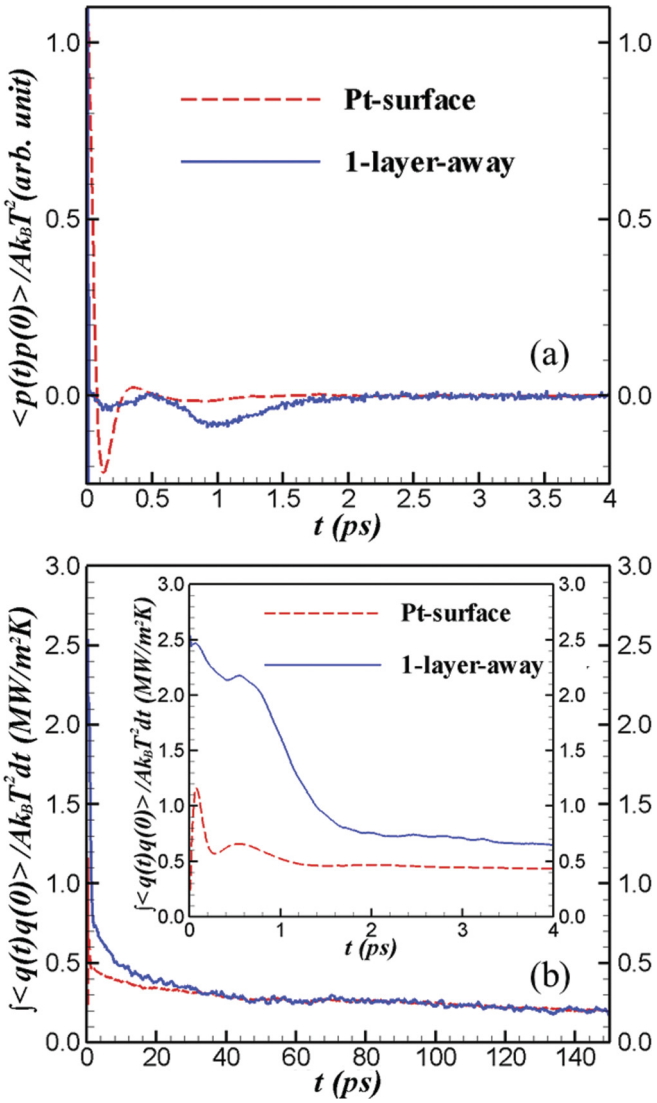

FIG. 4. (Color online) (a) Time correlation function of heat power across the solid-gas interface $\varepsilon_{sf} = 0.264 k_B T$. (b) Running integral of the time correlation function. The solid-gas interface is considered to be at the bare Pt surface or one adsorbed layer away from the Pt surface.

One is defined at the Pt surface ($z = 0$ Å where the gas density is zero) with Eq. (7) used for heat power calculation. The other is defined at a plane that is one adsorbed layer away ($z \approx 4$ Å where the gas density of almost the same as that of bulk gas) from the Pt surface, and Eq. (6) is used for heat power calculation. It is seen in Fig. 4(a) that the two time correlation functions are very different in the initial 2 ps, and both start to fluctuate around 0 after 2 ps.

The G_K is determined from the integral of the time correlation functions. The running integral of the initial 4 ps is shown in the inset of Fig. 4(b). Initially the running integral yields a plateau which can be used to determine G_K. However, we find it is difficult to evaluate G_K from the "plateau" because the running integral actually keeps decreasing after 2 ps. For instance, the running integral $\int \langle p(t)p(0)\rangle / A k_B T^2 dt$ decreases from 0.47 MW/m^{2}K at 2 ps to 0.38 MW/m^{2}K at 10 ps if the interface is defined at the Pt surface. Therefore, it is not possible to determine G_K unambiguously from the "plateau".

Instead of using the plateau, we use the tail of the running integral to determine G_K. As shown in Fig. 4(b), the two running integrals agree well with each other after initial 50 ps. The tail of the running integrals can be well fitted by exponential functions as shown in Fig. 5(a). The results are consistent with the prediction of Eq. (8). From the exponential fit, we find $G_{K,Pt}$ (interface defined at the Pt surface) and $G_{K,1\text{-layer}}$ (interface defined at one adsorbed layer away from the Pt surface) are 0.34 $\pm$ 0.03 MW/m^{2}K and

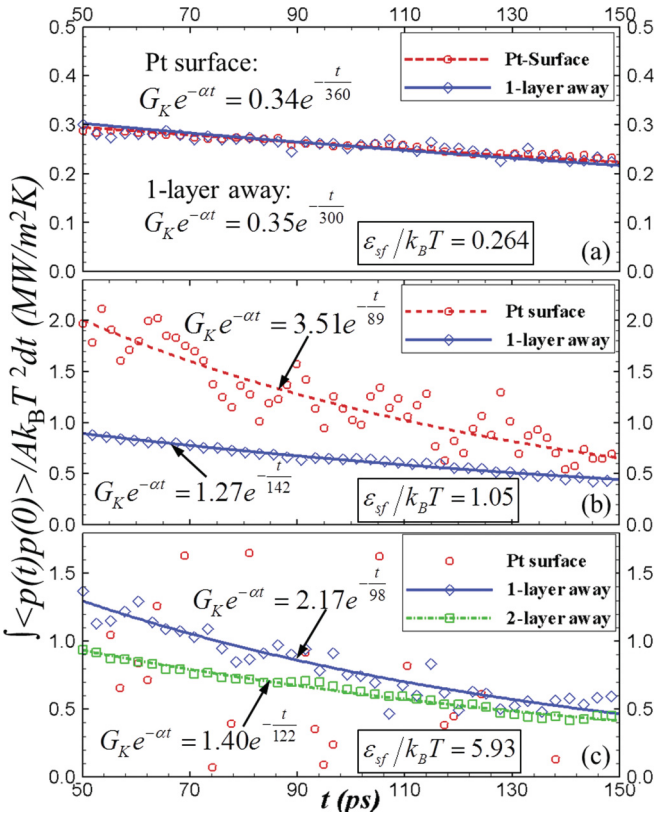

FIG. 5. (Color online) Exponential fit of the tail of the running integral $\int \langle p(t)p(0)\rangle / A k_B T^2 dt$ for $\varepsilon_{sf}/k_B T$ = (a) 0.264, (b) 1.05, and (c) 5.93.

0.35 ± 0.03 MW/m^{2}K, respectively. The result indicates that the effect of adsorbed layer in the case of $\varepsilon_{sf} = 0.264 k_B T$ is negligible.

As a comparison, we calculate G_K at the reference ε_{sf} from NEMD simulation. It is shown in Fig. 6(a) that G_K equals 0.39 ± 0.01 MW/m^{2}K, which agrees well with the EMD simulation result. According to Eq. (3), G_K of 0.39 ± 0.01 MW/m^{2}K corresponds to TAC of 0.45 ± 0.01. In addition, the TAC can be also determined directly from NEMD simulation using Eq. (2). We find TAC equals 0.44 ± 0.03 from Eq. (2).

The simulation is done at 300 K and 10 bar. Equations (3) and (4) indicate that G_K is proportional to collision rate, which is proportional to pressure. Therefore, the corresponding G_K at 1 atm and room temperature is about 0.04 MW/m^{2}K, which is 3 to 4 orders of magnitude smaller than the common solid-solid or solid-liquid interfacial thermal conductance.

C. Effect of adsorbed layers on G_K

Using the same method, we determine G_K at $\varepsilon_{sf} = 1.05 k_B T$. The EMD and NEMD simulation results are shown in Figs. 5(b) and 6(b), respectively. Upon the formation of an adsorbed gas layer, the appropriate definition of solid-gas interface is critical in the calculation of G_K's by the EMD method. As shown in Fig. 5(b), $G_{K,Pt}$ and $G_{K,1\text{-layer}}$ are 3.51 ± 0.20 MW/m^{2}K and 1.27 ± 0.07 MW/m^{2}K, respectively. It is notable that the $G_{K,Pt}$ is much larger than the theoretical maximum G_K (1.33 MW/m^{2}K). This is because the interface between the solid and adsorbed layer is more similar to a solid-liquid interface, which has a much larger thermal conductance. Consequently, it is seen in Fig. 6(b) that the temperature of the adsorbed layer is very close to the surface temperature in NEMD simulation. Hence, the solid-gas interfacial thermal resistance ($1/G_K$) is dominated by the thermal resistance at the interface between the adsorbed layer and the gas phase ($1/G_{K,1\text{-layer}}$), i.e., $G_K \approx G_{K,1\text{-layer}} = 1.27$ MW/m^{2}K.

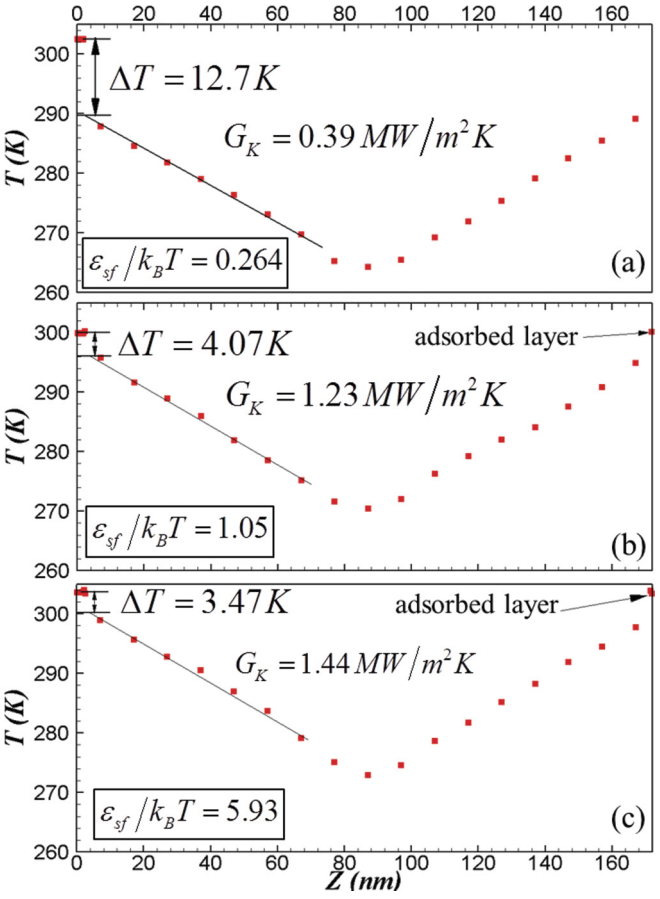

FIG. 6. (Color online) Temperature profile from NEMD simulation for $\varepsilon_{sf}/k_B T$ = (a) 0.264, (b) 1.05, and (c) 5.93.

For comparison G_K obtained from NEMD simulations [Fig. 6(b)] is 1.23 ± 0.09 MW/m^{2}K, which corresponds to TAC of 0.96 ± 0.04 according to Eq. (3), and which is essentially the same as TAC of 0.93 ± 0.02 calculated directly from Eq. (2). The above analysis indicates the solid-gas interface needs to be defined at one adsorbed layer away from the Pt surface to obtain the correct G_K from EMD simulation if an adsorbed layer is formed.

In the case of $\varepsilon_{sf} = 5.93 k_B T$, the second adsorbed layer is formed as depicted in Fig. 3(c). In the EMD determination of G_K, therefore, we also calculate $G_{K,2\text{-layer}}$ (interface defined at 7 Å, i.e., two adsorbed layers, away from the Pt surface) in addition to $G_{K,Pt}$ and $G_{K,1\text{-layer}}$. The corresponding EMD simulation results are shown in Fig. 5(c). While $G_{K,Pt}$ cannot be obtained from an exponential fit due to the too scattered data, the fitting results of $G_{K,1\text{-layer}}$ and $G_{K,2\text{-layer}}$ are 2.17 ± 0.15 MW/m^{2}K and 1.40 ± 0.12 MW/m^{2}K, respectively. As the second adsorbed layer is formed, $G_{K,1\text{-layer}}$ is much larger than the maximum theoretical G_K because the interface between the first and second adsorbed layers is also similar to a solid-liquid interface. Figure 6(c) shows the temperatures of the first and second adsorbed layers are both close to the surface temperature in the NEMD simulation. Therefore, the solid-gas interfacial thermal resistance is dominated by the thermal resistance at the interface between the second adsorbed layer and the gas phase, which means $G_K \approx G_{K,2\text{-layer}}$ = 1.40 ± 0.12 MW/m^{2}K.

For comparison, G_K obtained from NEMD simulation [Fig. 6(c)] is 1.44 ± 0.12 MW/m^{2}K, which corresponds to TAC of 1.04 ± 0.04, which furthermore agrees well with the TAC of 0.97 ± 0.06 calculated from Eq. (2). If solid-gas binding strength is strong enough to induce two adsorbed layers, therefore, the solid-gas interface needs to be defined at two adsorbed layers away from the Pt surface so as to obtain the correct G_K from EMD simulation.

We expect the third layer of gas atoms will be adsorbed on surface if the solid-gas interaction strength is further increased. In this case, the solid-gas interface should be defined at a plane out of the outmost adsorbed layer. However, further increase of solid-gas interaction strength is not realistic. Hence, we do not perform simulations at higher ε_{sf}.

D. Dependence of G_K and TAC on ε_{sf}

The G_K calculated from the EMD and NEMD simulations are summarized in Fig. 7. The figure shows the EMD and NEMD methods are equivalent in determination of solid-gas interfacial thermal conductance. The dependence of G_K on ε_{sf} in Fig. 7 is consistent with the dependence of solid-gas interaction time on ε_{sf} in Fig. 2. The interfacial thermal

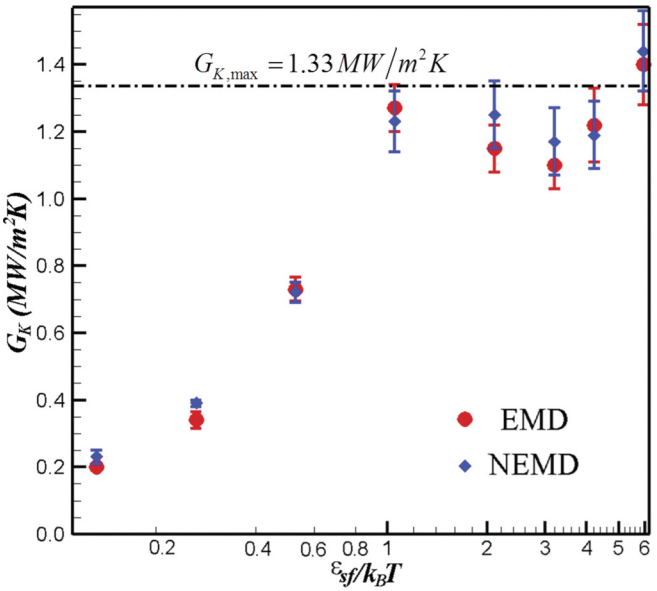

FIG. 7. (Color online) Solid-gas interfacial thermal conductance as a function of solid-gas binding strength ε_{sf} from EMD and NEMD simulations. The dashed line indicates the theoretical maximum G_K. The uncertainties are determined from the analysis of eight independent simulation runs.

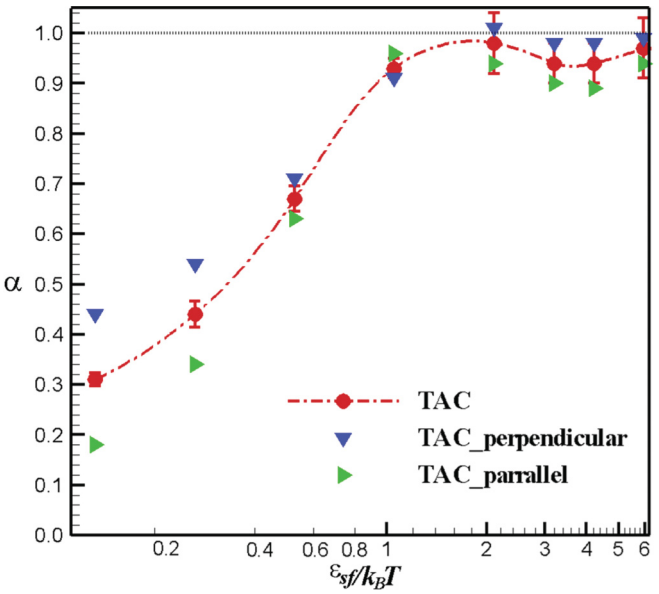

FIG. 8. (Color online) Thermal accommodation coefficient (total, perpendicular component, and parallel component) as a function of solid-gas binding strength ε_{sf}. The dashed-dotted line is used to guide the eye.

conductance does not reach the theoretical maximum G_K until the average solid-gas interaction time reaches about 150 ps. The result is consistent with the findings in Ar + Pt(111) molecular beam scattering experiments and simulations which show a complete thermalization of Ar requires over 100 ps [19]. If ε_{sf} is greater than $2k_BT$, gas phase atoms collide mostly with a softer adsorbed layer rather than with hard Pt surface. As the solid-gas thermal energy exchange is more efficient on a softer surface [3], it is reasonable to see the drop of G_K at $\varepsilon_{sf} = 3k_BT$ is not as significant as the drop of solid-gas interaction time at $\varepsilon_{sf} = 3k_BT$. The results in Figs. 2 and 7 indicate that complete thermalization of Ar with the Pt surface takes less than 50 ps if the surface is covered by adsorbed Ar atoms.

The dependence of TAC on ε_{sf} is shown in Fig. 8. The results are consistent with G_K in Fig. 7. At low ε_{sf}, there are almost no gas atoms adsorbed on the surface. The highly smooth Pt surface results in nearly conserved parallel momentum for any given collision [19]. Hence, the parallel component of TAC is much smaller than the perpendicular component. As the increase of ε_{sf}, a softer and corrugated gas layer is formed on the Pt surface. Accordingly, the difference between the parallel and perpendicular components of TAC becomes much smaller.

IV. CONCLUSION

In this work, solid-gas interfacial thermal conductance is calculated from EMD and NEMD simulations. EMD simulation results are found to be consistent with the NEMD simulation results. The appropriate definition of the solid-gas interface is critical in the correct determination of interfacial thermal conductance by the EMD method. If adsorbed layers are formed, the solid-gas interface should be defined at a plane out of the outmost adsorbed layer. An exponential fit of the tail of running integral $\int \langle p(t)p(0)\rangle / Ak_BT^2 dt$ is more reliable in the evaluation of interfacial thermal conductance. If the Pt surface is covered by adsorbed Ar atoms, we find that the incident gas atoms thermalize with the surface much more rapidly. Therefore, the adsorbed layer strongly affects the solid-gas interfacial heat transfer efficiency.

ACKNOWLEDGMENTS

This work is supported by the U.S. Air Force Office of Scientific Research Grant No. FA9550-12-1-0351. We would like to thank Meng Shen for useful discussions on the MD simulation, and thank the National Institute for Computational Science (NICS) for providing us supercomputer resources for MD simulations.

[1] L. Xue, P. Keblinski, S. R. Phillpot, S. U. S. Choi, and J. A. Eastman, J. Chem. Phys. **118**, 337 (2003).
[2] L. Xue, P. Keblinski, S. R. Phillpot, S. U. S. Choi, and J. A. Eastman, Int. J. Heat Mass Transf. **47**, 4277 (2004).
[3] Z. Liang, W. Evans, T. Desai, and P. Keblinski, Appl. Phys. Lett. **102**, 061907 (2013).
[4] Z.-Y. Ong and E. Pop, J. Appl. Phys. **108**, 103502 (2010).
[5] Y. Chalopin, K. Esfarjani, A. Henry, S. Volz, and G. Chen, Phys. Rev. B **85**, 195302 (2012).
[6] S. Merabia and K. Termentzidis, Phys. Rev. B **86**, 094303 (2012).
[7] J.-L. Barrat and F. Chiaruttini, Mol. Phys. **101**, 1605 (2003).

[8] S. Shenogin, P. Keblinski, D. Bedrov, and G. D. Smith, J. Chem. Phys. **124**, 014702 (2006).
[9] G. C. Maitland, M. Rigby, E. B. Smith, and W. A. Wakeham, *Intermolecular Forces: Their Origin and Determination* (Clarendon Press, Oxford, 1981).
[10] S. M. Foiles, M. I. Baskes, and M. S. Daw, Phys. Rev. B **33**, 7983 (1986).
[11] C. Wang, J. Chen, J. Shiomi, and S. Maruyama, Int. J. Therm. Sci. **46**, 1203 (2007).
[12] F. O. Goodman and H. Y. Wachman, *Dynamics of Gas-Surface Scattering* (Academic Press, New York, 1976), pp. 23–31.
[13] G. S. Springer, *Heat Transfer in Rarefied Gases* (Academic Press, New York, 1971), p. 164.
[14] S. C. Saxena and R. K. Joshi, *Thermal Accommodation and Adsorption Coefficients of Gases* (Hemisphere Publishing Corporation, New York, 1989), p. 5, 313.
[15] L. Puech, G. Bonfait, and B. Castaing, J. Low Temp. Phys. **62**, 315 (1986).
[16] D. Frenkel and B. Smit, *Understanding Molecular Simulation* (Academic Press, San Diego, 2002), p. 75.
[17] H. J. C. Berendsen, J. P. M. Postma, W. F. Van Gunsteren, A. Di Nola, and J. R. Haak, J. Chem. Phys. **81**, 3684 (1984).
[18] P. Jund and R. Jullien, Phys. Rev. B **59**, 13707 (1999).
[19] M. Head-Gordon, J. C. Tully, C. T. Rettner, C. B. Mullins, and D. J. Auerbach, J. Chem. Phys. **94**, 1516 (1991).